

# Elastic all-optical networks: a new paradigm enabled by the physical layer. How to optimize network performances?

Vittorio Curri, Mattia Cantono, Roberto Gaudino

DET, Politecnico di Torino, Italy, [www.optcom.polito.it](http://www.optcom.polito.it), [curri@polito.it](mailto:curri@polito.it)

**Abstract** *Physical layer equipment is the enabling technology for the elastic use of networks. We propose the statistical network assessment process as benchmarking method. As an example we compare PM-mQAM vs. TDHMF transceivers on a Pan-EU network topology, considering three fibers.*

## Introduction

Over the last decade, back-bone optical networks have deeply modified their nature. In legacy networks operated by direct-detection (DD) transceivers, node-to-node links were like sealed data pipe-lines, and optical-electric-optical (OEO) regeneration was needed at every node. Hence, transparency at the logical IP level did not meet similar characteristics at the optical transmission WDM level. With the development of DSP-based transceivers using multilevel modulation formats with coherent receivers and channel equalization<sup>1</sup>, network nodes may now route selected lightpaths (LPs) provided that they maintain the overall LP quality-of-transmission (QoT) above the in-service threshold. Hence, state-of-the-art optical networks are indeed transparent at every level, and the IP layer may operate logical links actually corresponding to physical LPs.

In such a novel scenario, every design-choice at the physical layer impact the network behavior. Such options are, among others, nodes' structure, transmission techniques, spectral use, fiber types, optical amplification and regenerators' placement. Hence, potentialities for transmission equipment expanded, but the quantitative derivation of its merit on network performances is not straightforward, because a holistic approach is now needed.

Besides enabling transparent wavelength routing, the use of DSP-based transceivers has dramatically simplified the link structure, removing the need for in-line dispersion-compensating units<sup>2</sup>. In this transmission scenario, the unique parameter for lightpaths' QoT is the generalized optical signal to noise ratio (OSNR), including the accumulation of both the ASE noise introduced by the amplifiers and the non-linear interference (NLI) generated by the Kerr effect in fiber propagation<sup>3</sup>.

Authoritative forecasts, e.g.,<sup>4</sup>, indicate for the IP traffic evolution a compound annual growth rate (CAGR) of 23% until 2019. Moreover, for the traffic in the busiest 60-minutes of the day – the busy-hour traffic – the envisioned CAGR is larger

than 30%. So, optical networks will have to increase both the average throughput capacity and the flexibility in time. It entails the implementation of the elastic all-optical networks paradigm.

On the other hand, network operators want to maximize the return on investments done on the already installed fibers and optical amplifiers<sup>5</sup>, limiting as much as possible the installation of new in-field equipment. Thus, they are starting to implement the elastic paradigm on fixed-grid WDM networks on the C-band, trying to maximize the link capacity over this band. Later on, they will eventually remove passive filtering components in nodes and will move to flex-grid transmission, at least for the dynamic busy-hour traffic. Such an evolution will require the adaptation of network management as well as selected hardware upgrades, having as constraints the fulfilment of IP traffic growth on one side, and the minimization of costs and of energy consumption, on the other.

Merit of transmission components for point-to-point capacity have been extensively analyzed, and fundamental limits have been established<sup>6</sup>. While a general assessment of networking merits of transmission solutions has not yet been developed. The method called Statistical Network Assessment Process (SNAP) has been recently proposed<sup>7,8</sup> to this purpose: it analyzes a progressive loading of networks according to a defined connectivity matrix and an established routing and wavelength assignment algorithm (RWA). SNAP can be applied starting from a completely unloaded network, or from a given connection status. SNAP makes use of a detailed modeling – the incoherent Gaussian-Noise model (IGN)<sup>3</sup> – for the physical layer and implements a Monte Carlo analysis (MCA). It derives the statistics of the metrics of interests, such as capacity, QoT and link saturation. So far<sup>7,8</sup>, SNAP has been applied to *static* traffic loading, starting from an unloaded network, but it can be easily ungraded in order to estimate the merit of dynamic – or burst-mode – transmission solutions.

Contrary to typical analyses aimed at deriving optimal solutions, given the traffic, SNAP delivers the statistics of network metrics. So, results can be read as the quantitative merit parameters of physical layer. SNAP shows also the weaknesses of networks, as, for instance, links' congestion, consequently addressing specific physical layer and/or RWA updates.

We shortly review SNAP and, as application examples, test different solutions for the elastic transceivers needed to implement the elastic paradigm in fixed-grid networks. We compare the use of pure PM-mQAM formats (PF) vs. time-division hybrid modulation formats (TDHMF)<sup>9</sup> on a pan-EU network topology, considering three fiber types. We propose the use of the average bit-rate ( $R_b$ ) per LP ( $R_{b,\lambda}$ ) as benchmark metric for the physical layer, obtained applying a QoT-based RWA. Finally, we discuss on how SNAP is able to point out network weaknesses and to address solutions.

### SNAP: a statistical study of network loading

Fig. 1 describes the studied Pan-EU network as a graph weighted by distances in km. Using the LOGO network-plane<sup>10,11</sup>, each LP QoT from node  $i$  to node  $j$  is given by the accumulated  $OSNR_{i,j}$  enabling the bit-rate  $R_b$ : the larger the  $OSNR$ , the larger the bit-rate<sup>9</sup>. Thanks to the use of the IGN<sup>3</sup>, the inverse  $OSNR$  ( $IOSNR_{i,j}=1/OSNR_{i,j}$ ) linearly adds-up as:

$$IOSNR_{i,j} = \sum_{\text{crossed links}} \Delta_{IOSNR,l} + \sum_{\text{crossed nodes}} \Delta_{IOSNR,n}, \quad (1),$$

where  $l$  and  $n$  identify the crossed links and nodes, respectively, connecting node  $i$  to node  $j$ , and  $\Delta_{IOSNR}$ 's are the  $IOSNR$  degradations. SNAP operates on the graph according to the Fig.3 flow-chart, requiring the following inputs.

1. The node-to-node LPs demands organized as the connection matrix. As an example, we use an *any-to-any* matrix and consider demands in terms of number of requested LPs, so we do not consider traffic grooming.
2. The initial network load: pre-allocated connections. In this work, we suppose to start SNAP on unloaded networks.
3. A description of the network topology including the physical layer (fiber types, amplifiers and spectral use) in order to compute the  $OSNR$  of each available LP.
4. The characteristics of the RWA: how LPs are ranked and consequently allocated. In this work, we use the strategy based on the  $k_{max}$  highest- $OSNR$  LPs with first-fit wavelength assignment. LPs are ranked according to their  $OSNR$ , and up to  $k_{max}$  of them are considered for allocation. The larger  $k_{max}$ , the larger the

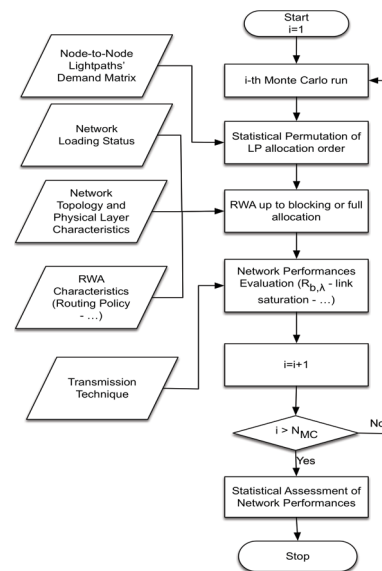


Fig. 2: Statistical Network Assessment Process

solution space of the RWA.

5. The transmission technique determining the maximum  $R_b$  per LP given its  $OSNR$ .

A Monte Carlo analysis (MCA) is then performed. During each MCA run, the set of LPs' demands is randomly shuffled to vary the order in which LPs' requests are progressively allocated, similarly to the waveplane method<sup>12,13</sup>. The RWA process terminates when all demands have been considered. Some will not be satisfied, resulting on a blocking percentage. Many metrics can be computed for each MCA run. Here, we consider

$$\text{the average } R_b \text{ per LP: } R_{b,\lambda} = \frac{1}{N_{L,i}} \sum_{j=1}^{N_{L,i}} R_{b,j} \quad \text{Gbps} \quad (2),$$

where  $N_{L,i}$  is the number of allocated LPs during the  $i$ -th run and  $R_{b,j}$  refers to the  $j$ -th LP. After the number of MCA iterations  $N_{MC}$  needed for convergence –  $N_{MC}=2500$  in this work – the probability density function (PDF) of metrics can be estimated, thus obtaining a statistical insight on network strengths and weaknesses.

### Results

As an example, we apply SNAP to the Pan-EU network of Fig. 2 with uniform amplified and uncompensated links. The use of three fiber types (NZDFS, SMF and PSCF) is compared, supposing to operate on the 50 GHz grid on the 4 THz C-band, with elastic transceivers running at  $R_s=32$  Gbaud gross symbol rate, including 28% FEC+signaling overhead. So, for PF-operated transceivers the net  $R_{b,\lambda}$  can be 50, 100, 200 or 300 Gbit/s, while TDHMFs enable to tune  $R_{b,\lambda}$  with continuity from 50 to 300 Gbit/s<sup>9</sup>, depending the LP  $OSNR$ .

Fig. 3 shows the PDF for  $R_{b,\lambda}$  obtained for the considered fibers using TDHMF transceivers.

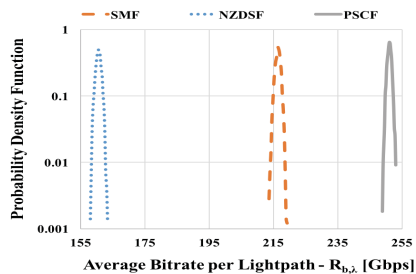


Fig. 3: PDF of  $R_{b,i}$  for the three considered fiber types

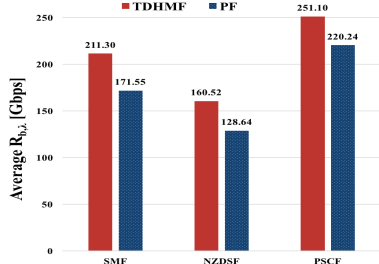


Fig. 4:  $\langle R_{b,i} \rangle$  for PF and TDHMF for the three fibers

As expected, PDFs are Gaussian-shaped, and the average  $\langle R_{b,i} \rangle$  is the parameter we use to quantitatively benchmark physical layer options. Also the  $R_{b,i}$  variances give useful information. They are related to the blocking, that grows with the dependence of RWA outcomes on the allocation orders. Hence, the larger the variance, the larger the space for investigations aimed at optimal LP allocations, given the traffic.

Fig. 4 summarizes the benchmarking results. For point-to-point transmission, the hierarchy among fibers is established<sup>14</sup>: PSCF first, SMF in the middle, and the NZDSF as last. This hierarchy holds also at the networking level, but the advantage of TDHMF vs. PF is indeed different fiber by fiber. For the SMF it is about 23%, for the PSCF is 15%, while it is about 24% for the NZDSF. The reason for a better effectiveness of TDHMF on NZDSF is the larger number of LPs with poor QoT experiencing a greater benefit from the continuity in  $R_b$  tuning. Fig. 5 shows a contour plot of links' spectrum utilization (SU) vs. the links' set and the  $k_{max}$  of the RWA. It shows the enhancement of SU enabled by a RWA with larger  $k_{max}$  that exploits poorer QoT LPs. Similar results are pictorially described in Fig. 6 on the network topology as width of graph edges: the thicker the edge, the higher the spectral use. From Fig. 6, one may deduce the most critical set of links within the network topology. From this knowledge, specifically targeted upgrades can be driven and tested. These may be related to the improvement of LP QoT as, for instance, the use of some Raman pumping and/or the placement of OEO regenerators. Alternatively, Fig. 6 may address bandwidth enlargement options, as the spatial division multiplexing (SDM) implemented by turning on selected dark fibers, if available, or by the C+L bandwidth extension.

## Conclusions

We have proposed SNAP as network analysis tool to benchmark different physical layer solutions needed to enable the transparency paradigm. As an example, we have tested SNAP on a Pan-EU WDM network topology showing the benefits of TDHMF vs. PF transceivers using three fiber types. We have also shown how SNAP is able to identify network weaknesses addressing specific physical layer or RWA solutions.

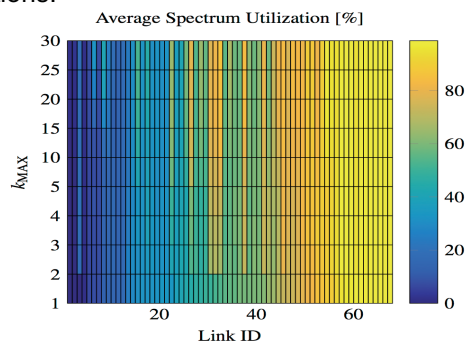


Fig. 5: Links' spectrum utilization with different  $k_{max}$

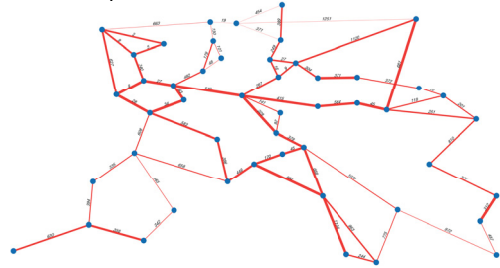


Fig. 6: Graphical representation of links' spectral use: the thicker the edge, the larger the spectral use.

## References

- [1] D.S. Ly-Gagnon *et al.*, "Coherent Detection of Optical Quadrature Phase-Shift Keying Signals With Carrier Phase Estimation," *JLT*, 24, pp. 12-21, 2006.
- [2] V. Curri *et al.*, "Dispersion compensation and mitigation of non-linear effects in 111 Gb/s WDM coherent PM-QPSK systems," *PTL*, 20, 1473-1475, 2008.
- [3] P. Poggiolini *et al.*, "The GN-Model of Fiber Non-Linear Propagation and its Applications," *JLT*, 32, p.694, 2014.
- [4] Cisco, "Cisco visual networking index: Forecast and methodology, 2014- 2019," Tech. Rep., May 2015.
- [5] G. Wellbrock, "How Will Optical Transport Deal With Future Network Traffic Growth?," ECOC 2014, Th.1.2.1.
- [6] Essiambre R.J. *et al.*, "Capacity Limits of Optical Fiber Networks," *JLT*, p.662, 2010.
- [7] M. Cantono *et al.*, "Data-rate figure of merit for physical layer in fixed-grid reconfigurable optical networks," OFC 2016, Tu3F.3.
- [8] M. Cantono *et al.*, "Potentialities and Criticalities of Flexible-Rate Transponders in DWDM networks: a Statistical Approach," to appear on JOCN.
- [9] F. Guimar *et al.* "Hybrid Modulation Formats Enabling Elastic Fixed-Grid Optical Network," to appear on JOCN.
- [10] P. Poggiolini *et al.*, "The LOGON strategy for low-complexity control plane implementation in new-generation flexible networks," OFC 2013, OW1H.3.
- [11] R. Pastorelli *et al.*, "Network Planning Strategies for Next-Generation Flexible Optical Networks," JOCN, 7, p. A511, 2015.
- [12] G. Shen, *et al.*, "Efficient heuristic algorithms for light-path routing and wavelength assignment in WDM networks under dynamically varying loads," *Comp. Comm.*, 24, p. 364, 2001.
- [13] H. Dai *et al.*, "Explore maximal potential capacity of WDM optical networks using time domain hybrid modulation technique," *JLT*, 33, p. 3815, 2015.
- [14] V. Curri *et al.*, "Design Strategies and Merit of System Parameters for Uniform Uncompensated Links Supporting Nyquist-WDM Transmission," *JLT*, 33, p. 3921, 2015.